5

Adaptation from Transmission Security (TRANSEC) to Cognitive Radio Communication

Chien-Hsing Liao and Tai-Kuo Woo
FooYin University/National Defence University
Taiwan (R.O.C.)

1. Introduction

Communication systems have to be made secure against unauthorized interception or against disruption or corruption in complicated electromagnetic environments. There are mainly three security categories used to delineate wireless communication systems generally, such as shown in Fig. 1, i.e., INFOSEC, COMSEC, and TRANSEC. We state about information security (INFOSEC) as that trying to against unauthorized access to or modification of information; we describe the communications security (COMSEC) as that keeping important communications secure. And we describe transmission security (TRANSEC) as that making it difficult for someone to intercept or interfere with communications without prior accurate waveforms, modulation schemes, and coding (Nicholson, 1987).

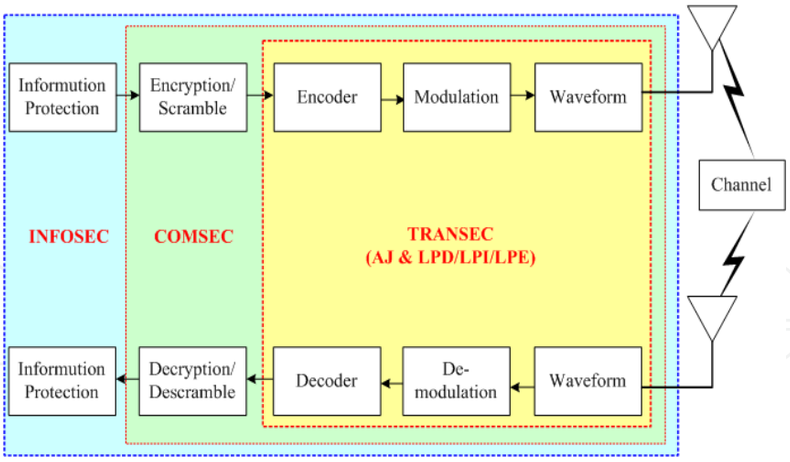

Fig. 1. Wireless communication security delineation

Therefore, in general, the basic strategies for acquiring and paralyzing the communication victim for the untended or intended users are to detect, intercept, exploit, and jam the communication signals. Relatively, the basic measures to counter these strategies for the victim are to design system with TRANSEC capabilities, i.e., low probability of detection, interception, and exploitation (LPD/I/E), and with receiving security capability, i.e., AJ or jam-resistant. LPD/I/E can be defined as measures with hidden signals which make it

difficult for the unintended or intended receivers to detect between signal plus noise and noise alone, to distinguish between the signals, and to abstract feature and recover message, respectively. Nevertheless, the requirements for AJ communications are almost directly opposite to those for LPD/I/E communications. For example, whenever communication system increases power to maintain communication distance and counter a jammer, it will increase the threat of being detected or even intercepted by an unintended interceptor receiver accordingly. On the other hand, whenever communication system decreases power to counter the threat of an interceptor, it will also unavoidably decrease the AJ capability. The same is true if power is replaced with many other system related parameters, e.g., antenna size.

In addition, the receiving and transmission security achieved by a communication link depends very strongly on its location relative to an adversary's jamming transmitter and intercept receiver, which is categorized as geometry-dependent factors. In AJ applications, it is very important to have an accurate estimation of the processing gain required for reliable communications as a function of the link geometry. In cases of LPD/I/E, the detection probability is significantly affected by the interaction of the link geometry and the relative locations of the intercept receiver and the communication transmitter. In geometric point of view, the central concept of TRANSEC secure communications, is trying to force the related jamming, detection, interception, or exploitation measures, to have to work within our prescribed region(s), e.g., physically dead zones or lethal zones, when in comparison with conventional communications, as shown in Fig. 2. (Schoolcraft, 1991) The inner red region represents conceptually the maximum range necessary for acquiring the TRANSEC communications signatures by the adversary side when in comparison with conventional communications in the outer yellow region. Similarly for AJ concerns, jamming has to approach furthermore into TRANEC communications region as well.

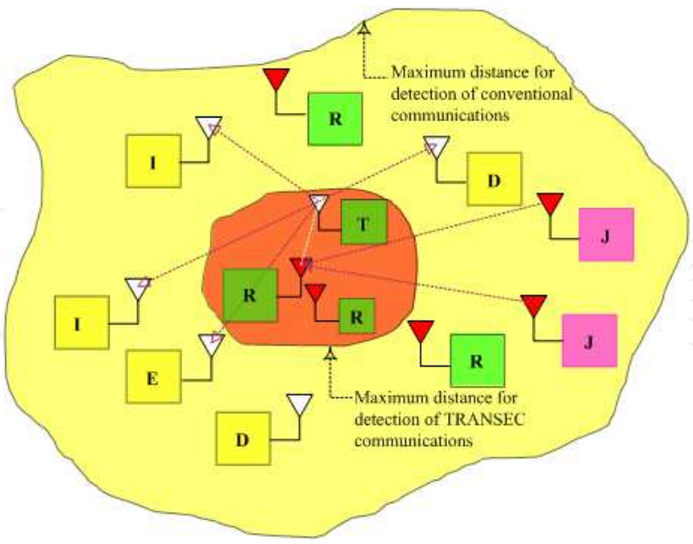

Fig. 2. TRANSEC communication scenario and concept

Under these circumstances as aforementioned, it is not straightforward to make wise and prudent evaluations and decisions for secure communications with concurrent AJ and LPD/I/E capabilities. Therefore, flexible and convenient metrics for achieving these are

expected. Moreover, how to get an analysis model and metrics of evaluating effectively a special type of jammer with real-time (or near concurrent) detection (passive scanning) and transmission capability (called repeater or follow-on jammer) for a frequency hopping (FH) communication system is also expected. Finally, based on these, spectrum sensing technique like this with real-time detection and transmission capability, especially for a cognitive radio (CR) FH communication, is also expected to be adapted and available for communication resources sensing. This chapter is organized as follows.

In Section 2, a systematic approach for evaluating the interactions of the link geometry and TRANSEC system parameters (AJ and LPD are assumed) for secure communication is proposed. In many typical cases, communication designs have to deal simultaneously with adversary threats of both active jamming and passive detection to protect against jamming and detection. And by increasing communication power to counter jammer and enhancing anti-jamming capability must be weighted carefully against the increased threats of deteriorating low probability of detection capability and being detected by an unintended interceptor receiver. A qualitative and quantitative approach with sinc-type antenna patterns being included for evaluating both AJ and LPD concurrently is reached. And it is intuitive to see that by spreading signal spectrum, complicating signal waveforms, and lowering power control uncertainty, respectively, will enhance system security and performance accordingly.

In Section 3, a cognitive radio unit (CRU) model with uniform scanning (U-scanning) and sequential scanning (S-scanning) techniques and cognitive perception ratio (CPR) metric for cognitive communications adapted from TRANSEC is investigated. In this model real-time spectrum sensing characteristics are coordinated together with system parameters in temporal and frequency domains, e.g., scanning rate and framing processing time, for evaluating the performance of the cognitive radio (CR) communications under an elliptical or a hyperbolic operation scenario. CR technology has been proved to be a tempting solution to promote spectrum efficiency and relieve spectrum scarcity problems. Nevertheless, the cognitive capability cannot only be realized by monitoring on some frequency bands of interest but also more innovative techniques are required to capture the spectrum holes with temporal, frequency or spatial variations in sophisticated Frequency hopping spread spectrum (FHSS) radio environments, and avoid interference to the existing primary users. Nowadays, the FHSS systems have been widely used in civil and military communications, but somewhat their benefits would be potentially neutralized by a follow-on jamming (FOJ) with wideband scanning and responsive jamming capabilities covering the hopping period. The FOJ concept is actually implicitly analogous to a CR communication with spectrum and location awareness, listen-then-act, and adaptation characteristics. High CPR value means high spectrum awareness but low coexistence. Many intriguing numerical results are also illustrated to examine their interrelationships.

In Section 4, a systematic approach with their corresponding metrics for evaluating independent and concurrent AJ and LPD performance qualitatively and quantitatively is drawn in this section. Moreover, specific scanning schemes and a quantified CPR metric are available for evaluations of the coexistence of radio resources. Section 5 is literatures listing.

2. Secure communications system through concurrent TRANSEC evaluations

The central concept for a secure communications system is to protect against unintended or intended jammers and interceptors, force them to change system parameters or work outside of the prescribed acceptable regions, and maintain secure system performance simultaneously. In this section, a systematic approach for evaluating the interactions of the link geometry and TRANSEC system parameters for secure communication will be investigated.

2.1 Survey of related works

There are many inspiring methods and metrics which have already been explored and proposed by many forerunners for secure communication related performance concerns, which are addressed as follows. Turner described the reasons of LPD/LPI/LPE communications developments and anti-jamming verse LPD/LPI/LPE communications requirements, which offer capabilities not available with AJ communications. The ideal characteristics of a LPD/LPI/LPE communications waveform and methods for detecting LPD/LPI/LPE transmissions are listed to form the basis for discussing of their developments and capabilities (Turner, 1991). Glenn made a LPI analysis and showed the effect of scenario-dependent parameters and detectability-threshold factors in jamming and non-jamming environments, and concluded that the most significant improvement in LPI performance can be obtained by operating at Extremely High Frequency (EHF) and by maximizing the effective spread-spectrum processing gain and the communicator's antenna discrimination to the jamming signal, and by minimizing the number of symbols in the message (Glenn, 1983). Based on power gains and losses, Gutman and Prescott have given a LPI system quality factor (Q_{LPI}) to a grouping of quality factor terms consisting of the antennas (Q_{ANT}), type of modulation (Q_{MOD}), atmospheric propagation conditions (Q_{ATM}), and interference rejection capability (Q_{ADA}) in the presence of jammers and intercept receivers (Gutman & Prescott, 1989). Based on gain difference between the communication receiver and the radiometer, Dillards developed a detectability gain (DG) metric for defining "acceptable" LPD performance of a communication signal by a radiometer, which includes their path losses, antenna gains, etc., plus two "mismatch" losses incurred by the radiometers (Dillard & Dillard, 2001). Using classical radiometer analysis and communication theory, Weeks et. al. developed a methodology through detectability distance to quantify the LPD characteristics of some COTS wireless communication systems, i.e., GSM, IS-54, IS-95, and WCDMA, which is obtained by exploiting the step-like function behavior of the probability of detection curve for a given system. Tradeoffs between the observation time of the interceptor and the detectability distance with multiple users are also investigated (Weeks et al, 1998). Mills and Prescott presented a scenario-independent stand-off intercept model for situations in which the collocated network transmitters and the relatively distant interceptor are assumed. Under these assumptions, the detectability performance of the network using a frequency hopping multiple access scheme (FHMA) can be evaluated for the wideband and channelized radiometers and LPI quality factors can be used to compare the performance of them (Mills & Prescott, 1995). Furthermore, Mills and Prescott also established two multiple access LPI network detectability models, i.e., scenario-independent standoff network and scenario-dependent dispersed network models, and developed their corresponding LPI performance metrics to provide new insight into these

issues (Mills & Prescott, 2000). Benia explored the effect of message length, processing gain, and coding gain on LPI performance and suggested a method for analyzing the effects of channel absorption loss models on the LPI quality factor (Binia, 2004). Wu investigated the impacts of the filter-bank interceptor performance and the emitter with FH waveform and specific antenna pattern on so-called circular equivalent vulnerable radius (CEVR) sensitivity within a statistical context like confidence interval (Wu, 2005).On the other hand, many forerunners have already investigated optimal interceptors for best detection probability concerns as well, which are addressed as follows. Schoolcraft defined six conventional and LPD waveforms to resist against seven detection techniques and provided a general approach to test the effectiveness of postulated threats against candidate waveforms and the relative LPD strengths of competing candidate waveforms (Schoolcraft, 1991). Wu studied the optimal interceptor for a FH-DPSK waveform, derived the detection algorithm based on the maximum likelihood principle, and proposed a novel performance evaluation approach (Wu, 2006). In spite of focusing on geometrical or power aspects of jamming only before, Burder analyzed and derived a mathematical intercept model for computation of the jamming probability when a follower jammer with a wideband-scanning receiver jams a single FH system (Burda, 2004). Gross and Chen developed and predicted the relative detection range for two types of transmitted waveforms, i.e., a benchmark rectangular pulse and a Welti binary coded waveform, and some classic passive receivers, e.g., square-law, delay and multiply, wideband, and channelized receivers possessing typical bandwidth, noise-floor, and loss parameters (Gross & Chen, 2005). In spite of the active jamming measures taken, FOJ is implicitly analogous to a cognitive radio communication with spectrum and location awareness, listen-then-act, and adaptation characteristics. For transmission security concerns, concurrent anti-jamming and low probability detection were investigated to have a secure communication (Liao et al., 2007).

2.2 System analysis scenario

The operation scenario with both AJ and LPD for a Ka-band GEO satellite communication system will be taken as system analysis model in this subsection. The relative geometry locations of the victim satellite communication system and the adversary multiple jammers and interceptors are shown in Fig. 3, where the victim communication terminal is put at the origin, and the latter two are collocated on the same fixed or varying positions, i.e., (x_1, y_1, 0), (x_2, y_2, 0), (x, y, 0), and (x_N, y_N, 0) etc. The paired jammer and interceptor on the same position (x, y, 0) are varying in an approaching or receding way for evaluating AJ and LPD performance. R_c is the range between our communication system themselves (e.g., R_c is assumed to be 36000kM for a geosynchronous elliptic orbit (GEO) satellite). R_j/R_i is the jammer/interceptor range from their collocated earth position to the victim communicator on the position of (0, 0, R). As shown in this figure, one very important factor for the effectiveness of jamming or interception is the relative angle φ off the main beam pattern of the victim communicator (on the position of (0, 0, R)) in the direction of earth jammer/interceptor. Generally, our friendly communication system (communicators at the origin and on the position (0, 0, R)) will direct main beam patterns at each other to get maximum gain patterns, and the intentional jammers or unintended interceptors will only be able to cover from the sidelobe direction, especially when the operating frequency is higher. Fig. 3 shows a basic scenario with an intercepted and jammed satellite and multiple jammers and interceptors on the ground. Whenever the jamming and interception range is

very far away from the victims, e.g., a GEO satellite, the interceptor and jammer will also get the advantage of the main beam gain of the victim communicator on the position (0, 0, R) relatively easier, if no antenna shaping or nulling pattern designs are taken.

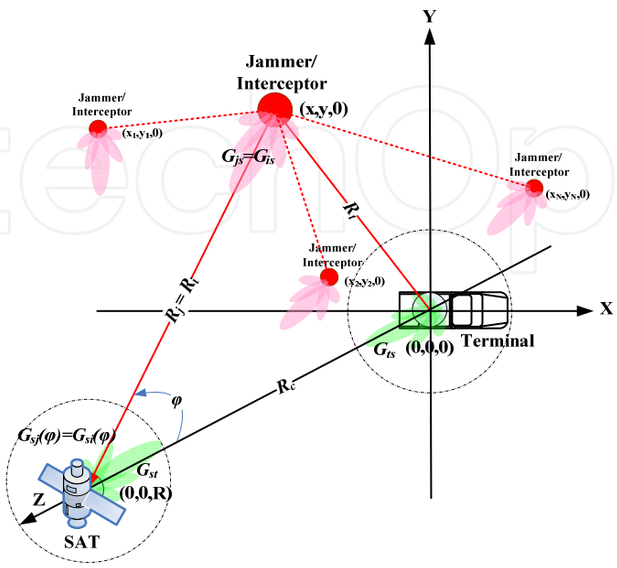

Fig. 3. The operation scenario with both AJ and LPD for a Ka-band GEO satellite communication system

Jammer/interceptor will get the advantages of the victim antenna pattern (mainlobe) to enhance their jamming or interception effects if the relative angles of the jammer/interceptor and the victim communicator on the position (0, 0, R) are tilted with the line of sight of the victim communicators themselves. The well-known parabolic antenna power gain $G_o(D)$ and pattern $G(\varphi)$ are given as follows (Jain, 1990)

$$G(\varphi) = \eta(\pi D/\lambda)^2 \left(\frac{2J_1(\pi D \sin(\varphi)/\lambda)}{\pi D \sin(\varphi)/\lambda} \right)^2, \quad (1)$$

where D is antenna diameter, λ is wavelength, η is antenna efficiency, and J_1 is first order Bessel function. If the satellite communicator on the position of (0, 0, R) is assumed to be the victim with a 3m sinc-type antenna, a narrower 30GHz and a wider 20GHz antenna patterns will be for uplink and downlink communication for the terminals on the ground, respectively. It is therefore good for anti-jamming design (30GHz) but not for LPD (20GHz) due to its wider transmission pattern.

2.3 Evaluation method

Not only are the power control schemes of a communication system very crucial to provide adaptive adjustments of transmission power and signal-to-noise ratios required, but are also the communication signal very dangerous to be more easily detected by the unintended or intended interceptors, especially, whenever the power sources are transmitted unscrupulously. In general, the receiving and transmission security achieved by a

communication link depends very strongly on its system related parameters and location relative to an adversary's jamming transmitter and intercept receiver, which can be categorized as system-dependent and geometry-dependent factors, respectively, for independent or concurrent AJ and LPD security concerns. The jamming to signal ratio (J/S) and the intercept signal to noise ratio $((S/N)_i)$ can be categorized, respectively, as system-dependent factors, i.e., f(•) and g(•) and geometry-dependent factors, i.e., $R_{js}(\bullet)$ and $R_{si}(\bullet)$, respectively. In coordination with the system operation scenario as shown in Fig. 3, the signal bit energy to jamming density (E_b/J_o), where J_o is very large compared to noise power density N_o, can be categorized as system-dependent factor h(•) and geometry-dependent factors $R_{ej}(\bullet)$, respectively. Furthermore, E_b/J_o can be proportionally or inversely related to these four system related parameters, i.e., processing gain (G_P), effective jamming power for the adversary jammer (ΔM_j), effective intercepting sensitivity for the adversary interceptor (ΔM_i), and effective power control for the victim communication system (ΔM_t). For example, whenever any of the latter three parameters is increased, E_b/J_o is lowered, i.e., error probability is increased. In contrast, whenever any of these three parameters is decreased, error probability is decreased.

2.4 Concurrent AJ and LPD communications (E_b/J_o)

In this subsection, in order to consider the AJ and LPD applications concurrently, we assume that the jamming power spectral density J_o is very large compared to noise power density N_o. Binary frequency shift keying (BFSK) is a kind of digital modulation method with two frequencies representing 0 and 1. Frequency hopping multiple access (FHMA) is a kind of spread spectrum schemes with many orthogonal or pseudo-orthogonal frequency patterns for multiple users application. The error probability for BFSK and FHMA combination, P_{fh}, is given by (Sklar, 2001)

$$P_{fh} \triangleq \frac{1}{2} \cdot e^{-\frac{1}{2}\left(\frac{E_b}{J_o}\right)}, \tag{2}$$

where E_b (=S/R_b) and J_o are, respectively, the bit energy and jamming power density given as follows for the n^{th} paired jammer/interceptor

$$J_{o,n} = P_{j,n} G_{js,n} G_{sj,n}(\varphi) \left(\frac{\lambda}{4\pi R_{j,n}}\right)^2 \frac{1}{W_{ss}} \quad J_{o,n} \gg N_o, \tag{3}$$

$$E_{b,n} = \frac{S_{t,n}}{R_b} = \left(\frac{S}{N}\right)_{io} \frac{G_{ts} G_{st}}{G_{ti,n}(\varphi) G_{it,n}} \frac{L_{i,n}}{L_t} \frac{N_{oi,n} W_{ss}}{R_b} \left(\frac{R_{i,n}}{R_c}\right)^2 \tag{4}$$

By substituting equation (3) and (4) into equation (2) and taking an inverse natural logarithm of it, the required E_b/J_o for the n^{th} paired jammer/interceptor is given as follows

$$\left(\frac{E_b}{J_o}\right)_n = \left(\frac{4\pi}{\lambda}\right)^2 \left(\frac{S}{N}\right)_{io} \left(\frac{G_{ts} G_{st} L_{i,n} N_{oi,n}}{G_{is,n} G_{js,n} G_{si,n}(\varphi) G_{sj,n}(\varphi)}\right) \frac{W_{ss}^2}{P_{j.n} R_b} \left(\frac{R_{i,n} R_{j,n}}{R_c}\right)^2, \tag{5}$$

$$\left(\frac{E_b}{J_o}\right)^{-1} = \sum_{n=1}^{N}\left(\frac{E_b}{J_o}\right)_n^{-1} \triangleq h(\bullet)R_{ej}(\bullet), \tag{6}$$

where $(S/N)_{io}$ means the optimum intercepting signal-to-noise ratio of an interceptor receiver; N_{oi} represents the output thermal noise power density of interceptor receiver, which is equal to $kT_0\ N_{fi,n}$, where k, T_0 and $N_{fi,n}$ are Boltzmann's constant (1.38×10^{-23} W/Hz/˚K), absolute temperature (290˚K assumed), and interceptor receiver noise figures, respectively. Equation (5) can also be categorized as system-dependent parameter h(•) and geometry-dependent parameters $R_{ej}(\bullet)$ as shown in equation (6). The E_b/J_o can be further manipulated and given as follows

$$\frac{E_b}{J_o} = \frac{(S/N)_{io}(S/N)_{to}G_P}{(J/S)(S/N)_i(S/N)_t}, \tag{7}$$

where G_p is the spreading spectrum processing gain given by W_{ss}/W_{bb} and $(S/N)_t$ is be given as follows

$$\left(\frac{S}{N}\right)_t = \frac{P_t G_{ts} G_{st}\left(\frac{\lambda}{4\pi|R_c|}\right)^2}{kT_o N_{ft} W_{bb} L_t} \tag{8}$$

From equation (7), J/S is inversely related to $(S/N)_i$ with the other parameters fixed, which can be further manipulated and simplified as given by

$$\frac{E_b}{J_o} = \frac{G_P}{\Delta M_j\ \Delta M_i\ \Delta M_t}, \tag{9}$$

where ΔM_j, ΔM_i, and ΔM_t are defined as J/S, $(S/N)_i/(S/N)_{io}$, and $(S/N)_t/(S/N)_{to}$, respectively. They mean the ratios of effective jamming power for the adversary jammer, effective intercepting sensitivity for the adversary interceptor, and effective power control for the victim communicator. E_b/J_o is inversely related to these three parameters if G_p is fixed. For example, whenever any of these three parameters is increased, E_b/J_o is lowered, i.e., error probability is increased. On the contrary, whenever any of these three parameters is decreased, error probability is decreased. From equation (9), it is intuitive for the victim communicator side to enhance system performance (lowering error probability) by spreading signal spectrum (G_p is increased), increasing signal power (ΔM_j is decreased), complicating signal waveforms (ΔM_i is decreased), and (or) lowering power control uncertainty (ΔM_t is decreased), respectively. For the adversary side, in order to deteriorate the performance of this secure victim communication system, ΔM_j, ΔM_i, and ΔM_t should be increased to lower E_b/J_o accordingly. In fact, the proposed concurrent AJ and LPD research can contribute to the CR communications for practical implementation by replacing all the collocated jammers/interceptors as shown in Fig. 3 with "cooperative" communicators, in which some geometry- and system-dependent factors can be sensed and aware of for spectrum resources adjustments or accesses, e.g., ΔM_j, ΔM_i, ΔM_t, relative positioning locations, and their corresponding parameters like power, bandwidth, spectrum hole, and etc.

2.5 E_b/J_o numerical analysis

In this section, one typical Ka-band (f_{up}/f_{dn}=30/20GHz) GEO satellite communication (SATCOM) example (R_c is assumed to be 36000kM) is illustrated through the proposed design approach for a secure communication system with concurrent requirements of both AJ and LPD capabilities. As shown in Fig. 3, the 7-m size jammer and interceptor antennas with maximum sinc type antenna pattern gains of G_{js} and G_{is}, respectively, are assumed in simulations. The antenna sizes for the communicators at the origin and on the position (0, 0, R) are both 3-m, and they are pointed each other with maximum gains. The sidelobe patterns leaked from the victim communicator on the position (0, 0, R) (i.e., GEO satellite) to the collocated interceptor and jammer on the ground are tilted φ angle dependent on relative positions among them, i.e., $G_{si}(\varphi)$ and $G_{sj}(\varphi)$. Based on equation (8) and (9) for concurrent AJ and LPD considerations, their corresponding figures of E_b/J_o verse R_t range for single or multiple collocated jammers/interceptors are shown in Fig. 4.

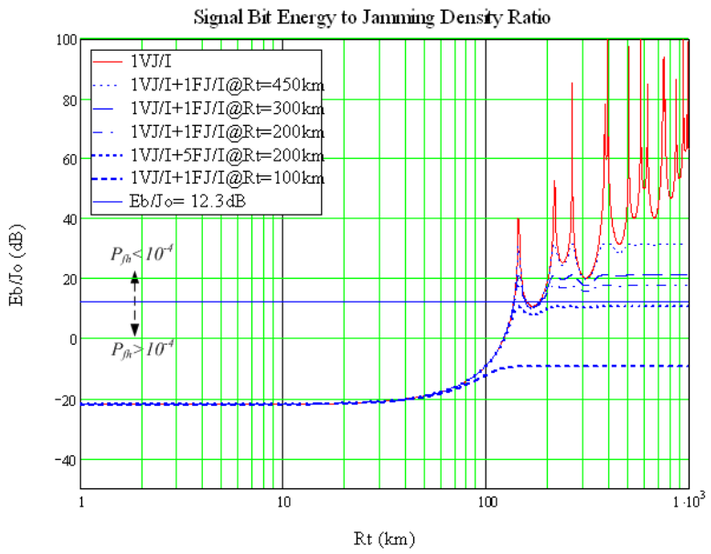

Fig. 4. Six different E_b/J_o ratios comparison with one varying collocated jammer/interceptor (VJI) and multiple collocated fixed jammer/interceptor (FJI) combinations

From Fig. 4, six different E_b/J_o ratios comparison with one varying collocated jammer/interceptor (VJI) and multiple collocated fixed jammer/interceptor (FJI) combinations are shown: 1 VJI(red solid—), 1 VJI + 1 FJI @R_t=450km(blue dot⋯), 1 VJI + 1 FJI @R_t =300km(blue dash----), 1 VJI + 1 FJI @R_t=200km(blue dash dot-·-·-), 1 VJI + 5 FJI @R_t=200km(thick blue dot⋯), and 1 VJI + 1 FJI @R_t=100km(thick blue dash----). The concurrent AJ and LPD performance under these single or multiple jammers/interceptors operation scenario can be examined if a minimum 10^{-4} FH error probability (P_{fh}) is asked to maintain (E_b/J_o=12.3dB). It is clear that whenever one single paired jammer/interceptor is beyond the range (R_t≈139kM), the communication performance criterion will be met ($P_{fh}<10^{-4}$) and not affected by this threat. Nevertheless, whenever under this operation scenario with one varying paired jammer/interceptor plus five jammers/interceptors all at R_t=200km, the specified communication criterion can not be met any more. For multiple fixed paired jammers/interceptors with one varying jammer/interceptor concerns, we find that there

exist even more "smoothed" effects for E_b/J_o curves when in comparison with J/S and $(S/N)_i$ curves as aforementioned, which maybe are due to randomized sidelobe patterns effects.

Fig. 5 shows the respective intuitive E_b/J_o contour plot with one varying jammer/interceptor and one collocated fixed jammer/interceptor (1FJI) at R_t=200km. The prescribed E_b/J_o=12.3dB circle (radius is about 139km) within which $P_{fh}>10^{-4}$ is also shown for concurrent AJ and LPD performance evaluations criterion. Therefore, a specific strategy could be taken to expel the approached varying jammer/interceptor beyond this zone. A much more smoothed E_b/J_o contour outside the prescribed criterion circle is observed, which means a less secure communication performance even only one more fixed jammer/interceptor at distant range is considered. According to equation (9), four main system-dependent factors can be as metrics for tradeoffs.

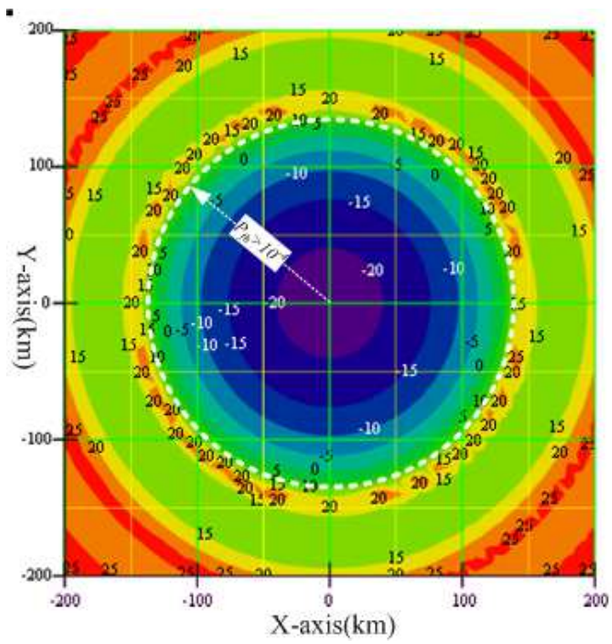

Fig. 5. E_b/J_o contour plot with one collocated varying jammer/interceptor (1VJI) and one collocated fixed jammer/interceptor (1FJI)

3. Spectrum sensing capability through specific scanning schemes

In previous section, we have proposed the approach of TRANSEC design by considering both AJ and LPE capabilities concurrently for multiple jammers and interceptors. In this section, we will further investigate a kind of special jamming with both real-time scanning and transmission characteristics, i.e., concurrent detection and jamming capabilities, which is designed inherently to counter a FH communication system. This should be a good bench target to evaluate the performance of the FH spread spectrum system with both transmission and reception characteristics being considered simultaneously. Moreover, effective jamming probability metrics for specified scanning schemes taken by FOJ, are investigated, which will be good figures of merit for evaluating FH and CR communication system performance.

3.1 Survey of related works

For the past years, traditional spectrum management approaches have been challenged by their actually inefficient use or low utilization of spectrums even with multiple allocations over many of the frequency bands (NTIA). Thus, within the current regulatory frameworks of communication, spectrum is a scarce resource ,Spectrum policy task force report, 2002). Cognitive radio is the latest emphasized technology that enables the spectrums to be used in a dynamic manner to relieve these problems. The term "cognitive radio (CR)" was first introduced in 1999 by Mitola and Maguire and is recognized as an enhancement of software defined radio (SDR), which could enhance the flexibility of personal wireless services through a new language called the *radio knowledge representation language* (RKRL), and the cognition cycle to parse these stimuli from outside world and to extract the available contextual cues necessary for the performance of its assigned tasks (Mitola III & Maguire Jr., 1999; Mitola III, 2000). Haykin therefore defines the cognitive radio as an intelligent wireless communication system that is aware of its surrounding environment, and uses the methodology of understanding-by-building to learn from the environment and adapt its internal states to statistical variations in the incoming *RF stimuli* by making corresponding changes in certain operating parameters in real-time (Haykin, 2005). In addition, some engineering views and advances for helping the implementation of cognitive radio properties into practical communications are described (Jondral & Karlsruhe, 2007; Mody et al., 2007). With these groundbreaking investigations and developments, international standardization organizations and industry alliances have already established standards and protocols for cognitive radio as well (Cordeiro et al., 2005; Ning et al., 2006; Cordeiro et al., 2006). The frequency hopping spread spectrum (FHSS) systems are widely used in civil and military communications, but somewhat the benefits of FHSS systems could be potentially neutralized by a follow-on jamming (FOJ) with an effective jamming ratio covering the hopping period (Torrieri, 1986; Felstead, 1998; Burda, 2004).

In spite of the active jamming measures taken, FOJ is implicitly analogous to a cognitive radio communication with spectrum and location awareness, listen-then-act, and adaptation characteristics. Therefore, the cognitive process cannot be simply realized by monitoring the power or signal-to-noise ratio in some frequency bands of interest in a FH radio environment. For transmission security concerns, concurrent anti-jamming and low probability detection were investigated to have a secure communication (Liao et al., 2007). Furthermore, real-time spectrum sweeping characteristics are coordinated together with system parameters in temporal and frequency domains, e.g., scanning rate and framing processing time, for evaluating the performance of CR communications under an elliptical or a hyperbolic operation scenario, which can be applied for radio spectrum sensing and location awareness in cognitive radio communications. The proposed schemes and metrics can pave one practical way for system evaluations of cognitive radio communications (Liao et al., 2009). Although the performance evaluation of cognitive radio (CR) networks is an important problem, it has received limited attention from the CR community. It is imperative for cognitive radio network designers to have a firm understanding of the interrelationships among goals, performance metrics, utility functions, link/network performance, and operating environments. Various performance metrics at the node, network, and application levels are reviewed. A radio environment map-based scenario-driven testing (REM-SDT) for thorough performance evaluation of cognitive radios and an

IEEE 802.22 WRAN cognitive engine testbed are also presented to provide further insights into this important problem area, respectively (Zhao et al., 2009). A coexistence window inside which the primary user and secondary user share the radio channel in time division manner is proposed. Connectivity probability and link utility efficiency are defined to measure the performance of secondary user. Considering the practical noise channel, how the metrics change is studied and the data rate of the secondary user in this case is obtained (Liu et al., 2010). An optimal power allocation scheme for a physical layer network coding relay based secondary user (SU) communication in cognitive radio networks is proposed. SUs are located on two different primary user (PU) coverage areas and an energy and spectrally efficient SU communication scheme is introduced (Jayasinghe et al., 2011). Finally, a latest systematic overview on CR networking and communications by looking at the key functions of the physical (PHY), medium access control (MAC), and network layers involved in a CR design and how these layers are crossly related are proposed, which can help researchers and practitioners have a clear cross-layer view on designing CRNs (Liang et al., 2011).

3.2 Model for FH jamming probability

Fig. 7 shows the basic FOJ function block diagram with many allocated process time to acquire incoming "victim" signals and implement jamming, where jT_z time is the total analytical time needed to acquire the instant hoping frequency, τ_r is the total activation time needed to synthesize and amplify a repeater signal tone or noise to jam the "victim" signal, which may compose of the process times of frequency synthesizer, power amplifier, and filter banks.

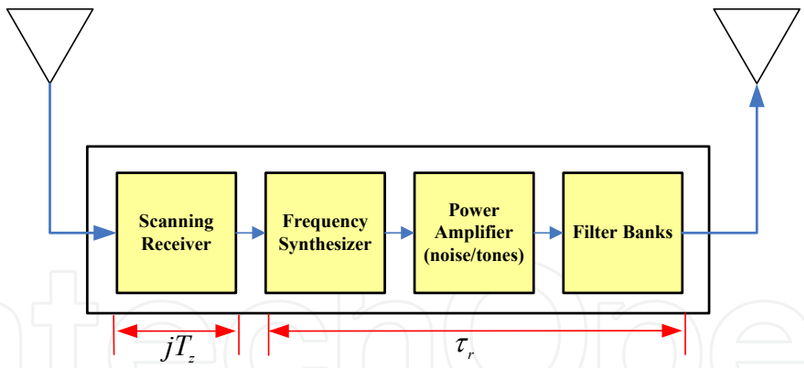

Fig. 6. Basic FOJ function block diagram

In general, the processed times for these three parameters are in the order of us, ns, and ns, respectively. Furthermore, the propagation delay or difference time (τ_d) dependent on relative positions should be included for effective jamming probability analysis. For example, if the range difference (ΔR) is 30km, the τ_d propagation difference time will be around 100 μs, far longer than the response time τ_r. Therefore, this parameter can be assumed to be zero while compared to other larger parameters under this circumstance.

Fig. 8 shows the effective jamming dwell time breakdown for FOJ, where T_r represents the jamming total delay time of process delay and propagation time ($=\tau_r+\tau_d$), T_l represents the latency time ($=jT_z + T_r$), and T_j represents the effective jamming dwell time ($=T_h-T_l$).

$$T_l = jT_z + \left(\tau_r + \Delta\tau_d\right) = jT_z + T_r\,, \tag{10}$$

$$T_J = T_h - \left(jT_z + T_r\right) = T_t - jT_z \tag{11}$$

T_j must be smaller than T_h under any circumstance. The effective jamming probability (h) is defined to be the ratio of T_j and T_h.

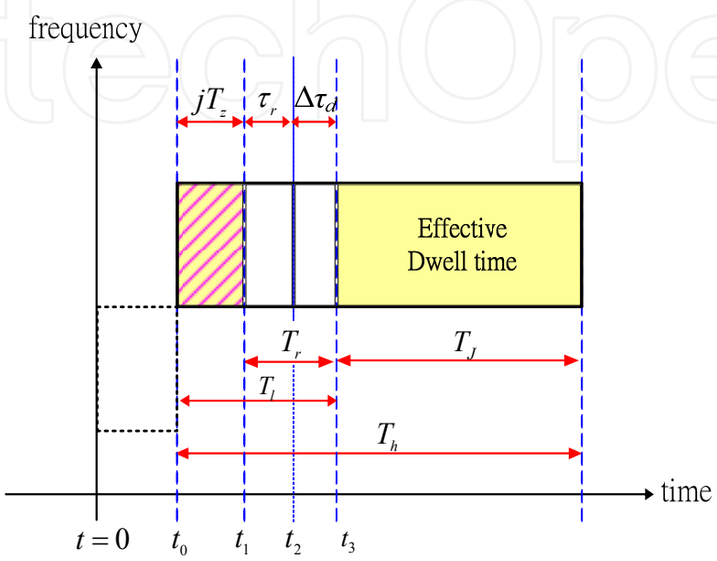

Fig. 7. Effective dwell time (T_J) and latency time breakdown for CRU operation

Scanning windows available during hopping dwell interval is defined to be m, which is represented as

$$m = \left\lfloor \frac{T_h - T_r}{T_z} \right\rfloor = \left\lfloor \frac{T_t}{T_z} \right\rfloor, \tag{12}$$

where T_z represents the analysis framing time per scanning window W_s of the jammer and $\lfloor x \rfloor$ symbol means the maximum integer equal to or smaller than x. It follows that the follower jammer is able to analyze at most m scan windows during the single dwell interval, T_h. Scanning window number available in the FH system bandwidth is defined to be n and represented as

$$n = \left\lceil \frac{W}{W_s} \right\rceil, \tag{13}$$

where W represents the hopping bandwidth of a FH system, W_s represents scanning window of the jammer, and $\lceil x \rceil$ symbol means the minimum integer equal to or larger than x. Let k be the number of scan windows which the FOJ analyzes in the dwell interval. It is evident that

$$k = \min(m, n)\,, \tag{14}$$

which means the smaller one of m or n is selected as the analyzed number of scanned windows. Let us suppose that one FH system operates in the bandwidth W only and that the follower jammer knows the parameters of the FH system and knows the moments of channel changes as well. Therefore, exactly at these moments (t=0), the jammer will initiate searching of the actual channel. When FH terminal transmits in j^{th} scan window, then this transmission is found at moment $t_0 = jT_z$. Let t_1 be the moment when the scanning receiver finds the actual transmission channel of the FH system. Let t_2 be the moment when the follower jammer initiates jamming of the found channel. Let t_3 be the moment when the initiated signal of the FOJ reaches the receiver site of the found channel, i.e., the FH receiver is jammed at the moment t_3.

3.3 Scanning schemes

In the following sections, two schemes named uniform scanning and sequential scanning will be explored and taken as scanning measures to scan and trace the incoming hopping signals fast enough to implant effective noise or tone jamming thereafter. In addition, the case of delay response ($T_r \neq 0$) will be examined as well for these two scanning schemes.

3.3.1 Uniform scanning (U-scanning) scheme

A uniform scanning (U-scanning) technique will be explored and taken as the scanning measures to scan and trace the incoming hopping signals fast enough to implant transmission signals thereafter. If the CRU analyzes all scan windows randomly with uniform probability $p_u(T_J)=1/n$, and $p_u(T_J)=(n-k)/n$ is the probability that the FH system operates in the scanning window which is not analyzed. Therefore, the probability distribution of the jammed period of the dwell interval can be given by

$$p_u(T_J) = \begin{cases} \dfrac{(n-k)}{n}, & j > k\left(T_J = 0\right) \\ \dfrac{1}{n}, & j = 1,2,...k \end{cases} \tag{15}$$

It is assumed that T_r is assumed not to be zero, i.e., τ_r is zero, but τ_d is not zero and $T_r=\tau_d=l\times T_h$, where l is the propagation time ratio between $T_r = \tau_d$ and T_h. The average jammed period of the dwell interval is therefore derived and given by

$$\overline{T}_{Ju} = \sum_{j=1}^{n} T_J \cdot p_u\left(T_j\right) = \frac{k}{n}\left(\left(1-l\right)T_{hu} - T_z\frac{k+1}{2}\right) \tag{16}$$

From the above derived equation, the criterion of hopping rate (R_{hu}) and analysis framing time product (T_z) for effective dwell can be available and given by

$$R_{hu} \cdot T_z \le \left(1-l\right)\cdot\frac{2}{\left(k+1\right)}, \tag{17}$$

which is the basic condition whenever $T_r \neq 0$ for effective CRU. The effective dwell ratio and scanning rate (R_{su}) for uniform scanning technique can be expressed and given by equation (18) and (19), respectively.

$$h_u = \frac{\overline{T}_J}{T_h} = \frac{k}{n} \cdot \left((1 - l) - \frac{T_z}{T_h} \frac{k+1}{2} \right), \tag{18}$$

$$R_{su} = \frac{W_s}{T_z} = W_s \cdot R_{hu} \cdot \left(\frac{k(k+1)}{2 \cdot \left((1 - l) \cdot k - n h_u \right)} \right) \tag{19}$$

3.3.2 Sequential scanning (S-scanning) scheme

A sequential scanning scheme will be taken as the scanning measure to scan the incoming frequency hopping signals fast enough to implant CRU transmit signal if it is allowable. Based on the basic definitions as aforementioned, if CRU analyzes all scanning windows randomly with sequential perception $p_s(T_J)=1/(n+1-j)$, then $p_s(T_J)=(n-k)/(n+1-j)$ will be the perception not analyzed in the scanning window. Therefore, the perception distribution of the effective dwell time can be given by

$$p_s\left(T_J\right) = \begin{cases} \dfrac{n - k}{n + 1 - j}, & j > k\left(T_J = 0\right) \\ \dfrac{1}{n + 1 - j}, & j = 1, 2, \ldots, k \end{cases} \tag{20}$$

It is assumed that T_r is assumed not zero and $T_r=\tau_r+\Delta\tau_d=l\times T_h$, where l is the propagation time ratio between T_r and T_h. The average effective dwell time can therefore be derived and given by

$$\overline{T}_{Js} = \sum_{j=1}^{k} T_J \cdot p_s\left(T_j\right) = \sum_{j=1}^{k} \left(\frac{(1 - l) \cdot T_{hs} - j T_z}{n + 1 - j} \right) \tag{21}$$

From (21), the criterion of hopping rate ($R_{hs}=1/T_{hs}$) and framing processing time product (T_z) for effective dwell time can be available and given by

$$R_{hs} \cdot T_z \le \frac{\sum_{j=1}^{k} \left(\dfrac{1 - l}{n + 1 - j} \right)}{\sum_{j=1}^{k} \left(\dfrac{j}{n + 1 - j} \right)}, \tag{22}$$

which is the basic criterion whenever $T_r \neq 0$ for effective coverage of the hopping period. Therefore, the effective dwell time ratio and the scanning rate by sequential scanning scheme can be manipulated further and given by equation (23) and (24), respectively.

$$h_s = \frac{\overline{T}_J}{T_h} = \sum_{j=1}^{k} \left(\frac{1 - l}{n + 1 - j} \right) - \frac{T_z}{T_{hs}} \cdot \sum_{j=1}^{k} \left(\frac{j}{n + 1 - j} \right), \tag{23}$$

$$R_{sh} = \frac{W_s}{T_z} = W_s \cdot R_{hs} \cdot \left(\frac{\sum_{j=1}^{k} \left(\frac{j}{n+1-j} \right)}{\sum_{j=1}^{k} \left(\frac{1-l}{n+1-j} \right) - h_s} \right) \tag{24}$$

3.4 Geometric model for FH jamming

In this section, two analytical geometric models, i.e., elliptic and hyperbolic, will be examined furthermore dependent on their relative positions among the FOJ, FH transmitter, and FH receiver.

3.4.1 Elliptical FH jamming model

Fig. 9 shows an elliptic FH jamming model. If the relative positions among the FOJ, FH transmitter, and FH receiver are shown in Fig. 9 with fixed range R_{tr}=a between the FH transmitter and receiver and varying FOJ position, then the following expressions will be available by using the fact that latency time (T_l) should be smaller than the hopping period (T_h) for an effective jamming.

$$T_l = jT_z + \tau_r + \tau_d = jT_z + \tau_r + \frac{\left(R_{tj} + R_{jr} - a \right)}{c} \le T_h \,, \tag{25}$$

where τ_r can be assumed to be zero for instant response for the jammer, R_{jr} is the range between transmitter and FOJ, and R_{jr} is the range between FOJ and receiver.

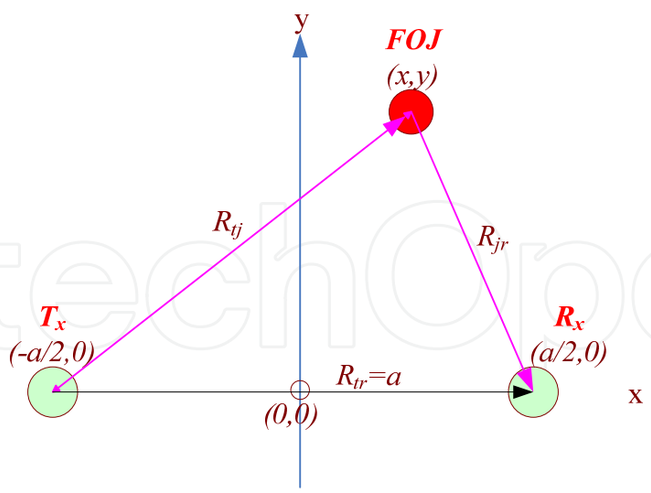

Fig. 8. Elliptic FH jamming model

After a simple manipulation, a standard ellipse equation will be given by

$$\frac{x^2}{(D+a)^2} + \frac{y^2}{D \times (D+2a)} = \frac{1}{4}, \tag{26}$$

where D is assumed to be given by

$$\left(R_{tj} + R_{jr} - a\right) \le \left(T_h - jT_z - \tau_r\right) \cdot c = D \tag{27}$$

Fig. 10 shows the typical hopping rate (R_h) contours for an elliptic FH jamming model with varying FOJ locations and assumed scanning time around 1ms (jT_z=10×100μs) and fixed R_{tr}=a =100km. Whenever a specified fixed hopping rate is required (e.g. R_h=500Hz), an even higher hopping rate is necessary for the FH communication system if FOJ is penetrated through this boundary and inside the specified ellipse. On the contrary, if FOJ is located outside the ellipse boundary, then the specified hopping rate is fast enough to counter the FOJ jamming for the FH communication system.

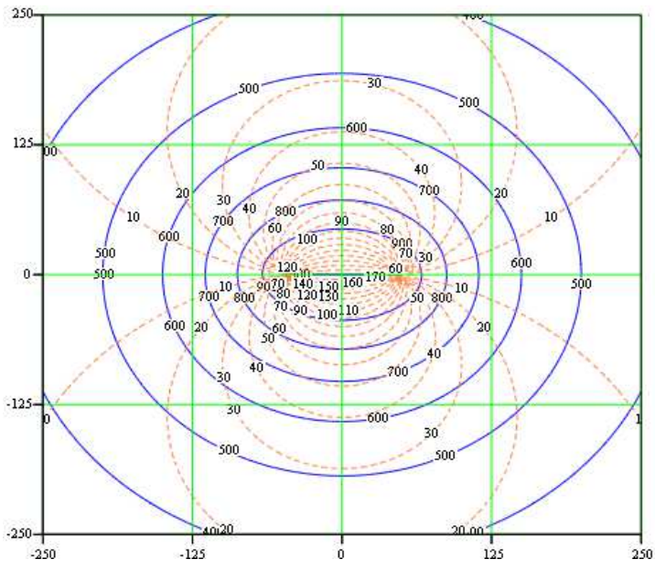

Fig. 9. Typical elliptic contour of FH jamming model

3.4.2 Hyperbolic FH jamming model

If the relative positions among the FOJ, FH transmitter, and FH receiver are shown in Fig. 11 with fixed range R_{tj}=a between the FH transmitter and FOJ and varying FH receiver position, then the following expressions will be available by using the fact that latency time (T_l) should be smaller than the hopping period (T_h) for an effective jamming.

$$T_l = jT_z + \tau_r + \tau_d = jT_z + \tau_r + \frac{\left(a + R_{jr} - R_{tr}\right)}{c} \le T_h\,, \tag{28}$$

where τ_r can be assumed to be zero for instant response for the jammer, R_{jr} is the range between FOJ and receiver, and R_{tr} is the range between transmitter and receiver. After a simple manipulation, a standard ellipse equation will be given by

$$\frac{x^2}{\left(D - a\right)^2} - \frac{y^2}{D \cdot \left(2a - D\right)} \ge \frac{1}{4}\,, \tag{29}$$

where D is assumed to be given by

$$\left(a+R_{jr}-R_{tr}\right)\le\left(T_h-jT_z-\tau_r\right)\cdot c=D\,, \tag{30}$$

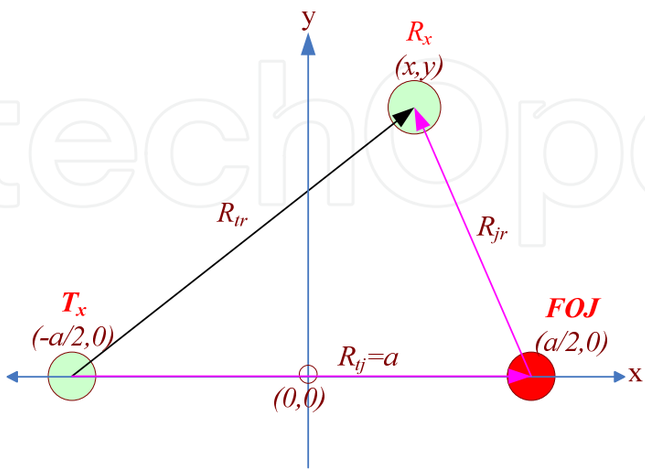

Fig. 10. Hyperbolic FH jamming model

Fig. 12 shows the typical contours for a hyperbolic FH jamming model with varying FH receiver locations and assumed scanning time around 1ms (jT_z=10×100μs) and fixed R_{tj}=a=100km. Whenever a specified fixed hopping rate is required (e.g. R_h=650Hz) under this circumstance, an even higher hopping rate is necessary for the FH communication system if the varying FH receiver is penetrated through this boundary to be closer to the fixed FOJ position on the right side. On the contrary, if the varying FH receiver is located on the left side of the hyperbolic boundary, then the specified hopping rate is fast enough to counter the FOJ jamming for the FH communication system.

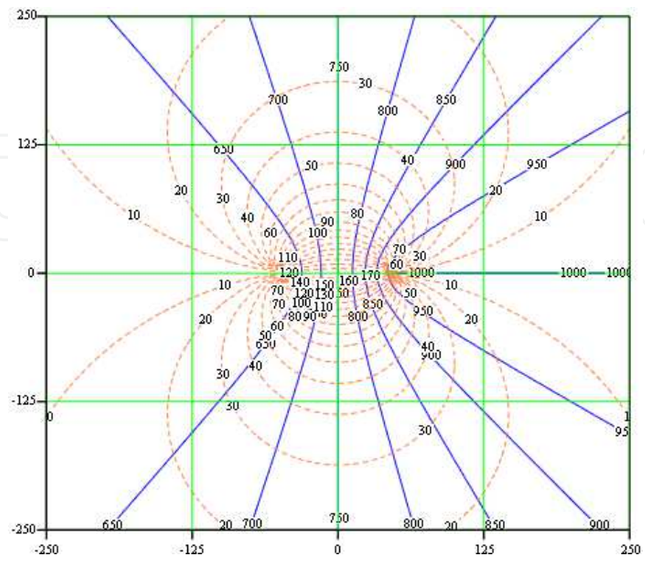

Fig. 11. Typical hyperbolic contour of FH jamming model

Fig. 13 shows the comparison results of effective jamming probability (h) vs. hopping rate (R_h) for both uniform (U-) scanning and sequential (S-) scanning schemes. Under the same framing time (T_z) conditions it is observed obviously that S-scanning scheme is better than U-scanning scheme for fixed hopping rate, e.g., the effective jamming probability value will be around 0.8 and 0.5 if R_h=500Hz and T_z= 100us for S- and U-scanning scheme, respectively. In another point of view, S-scanning scheme will have better hopping rate sensing capability (650Hz) than U-scanning scheme (500Hz) if effective jamming probability is fixed at 0.5.

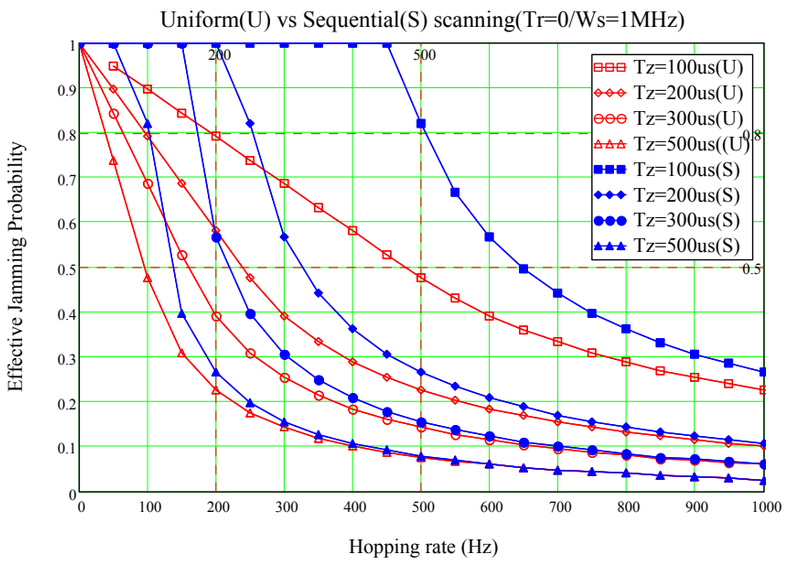

Fig. 12. Effective jamming probability vs. hopping rate with specified T_z values

3.5 Cognitive radio unit (CRU) and cognitive perception ratio (CPR)

Fig. 7 shows the basic FOJ function block diagram with many allocated process time to acquire incoming "victim" signals and implement jamming. This function block diagram is basically analogous to a cognitive radio unit (CRU) for sensing spectrum signals while applied in a cognitive communications adapted from TRANSEC. In addition, CRU models with U-scanning and S-scanning schemes and cognitive perception ratio (CPR) metric for quantified cognitive communications could be available as well. In this model real-time spectrum sensing characteristics can be coordinated together with system parameters in temporal and frequency domains, e.g., scanning rate and framing processing time, for evaluating the performance of CR communications under an elliptical or a hyperbolic operation scenario. Fig. 14 and Fig. 15 show the hyperbolic and elliptic CPR contours, respectively, with both U- and S-scanning being put together for comparisons, and with T_z=100us and R_h= 500Hz.

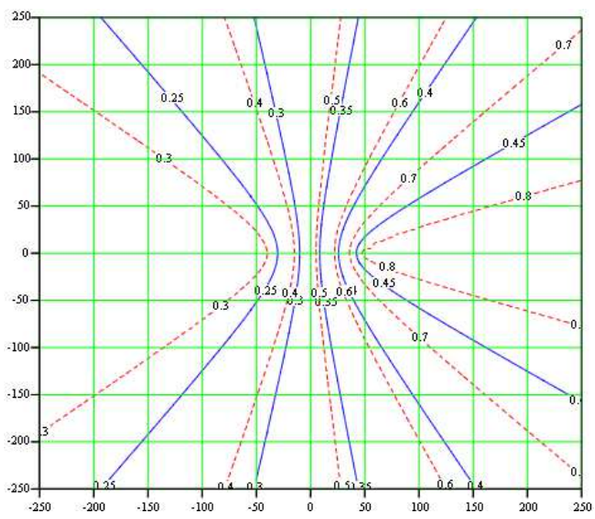

Fig. 13. Hyperbolic CPR contours with U- and S-scanning & R_h= 500Hz

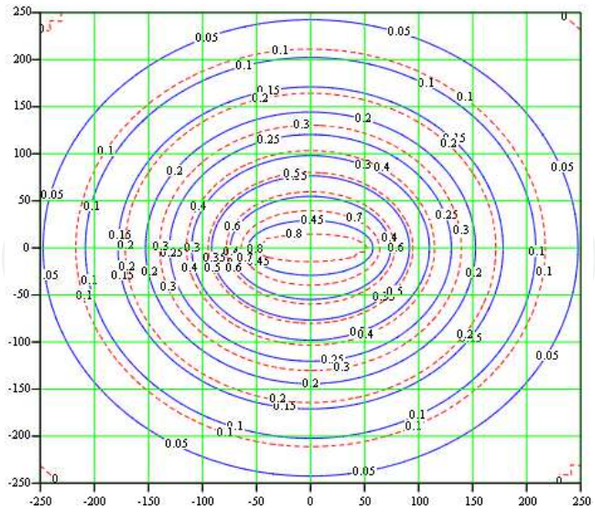

Fig. 14. Elliptic CPR contours with U & S scanning & R_h= 500Hz

It is observed from Fig. 14 that the CPR-contour values of 0.25 to 0.45 (blue solid) and values of 0.3 to 0.8 (red dashed) for U-scanning and S-scanning, respectively, are shown from the left hyperbolic trajectories to the right trajectories. And it is observed from Fig. 15 that the CPR-contour values of 0.05 to 0.45 (blue solid) and values of 0.1 to 0.8 (red dashed) for U-scanning and S-scanning, respectively, are shown from the outside elliptic trajectories to the inner trajectories. As stated in last section, the performance of S-scanning scheme is better than U-scanning scheme in many aspects. And it will be the same, if the location awareness conditions are established through direction finding and emitter location capability, and are collaborated with each other among CRUs.

4. Conclusion

In this paper, we have first proposed a systematic approach with their corresponding metrics for evaluating independent and concurrent AJ and LPD performance qualitatively and quantitatively. A representative GEO satellite communication scenario for independent and concurrent AJ and LPD performance evaluations is explored thoroughly. Based on these metrics, it is direct to see that by spreading signal spectrum, complicating signal waveforms, or lowering power control uncertainty, respectively, will enhance system performance accordingly. A CRU model with U-scanning or S-scanning techniques and a quantified CPR metric for cognitive communications adapted from TRANSEC is investigated as well. In this model real-time spectrum sensing characteristics are coordinated together with system parameters in temporal and frequency domains, e.g., scanning rate and framing processing time, for evaluating the performance of CR communications under an elliptical or a hyperbolic operation scenario, which can be applied for radio spectrum sensing and location awareness in cognitive radio communications. The proposed schemes and metrics can pave one practical way for the system evaluations of cognitive radio communications.

5. References

Nicholson, D. L. (1987). Spread Spectrum Signal Design-LPE & AJ systems, *Computer science Press*, 1987

Schoolcraft, R. (1991). Low Probability of Detection Communications-Waveform Design and Detection Techniques, *IEEE Military Communications Conference*, Vol. 2, pp. 832-840, November 1991

Jain, P. C. (1990). Architectural Trends in Military Satellite Communications Systems, *Proceedings of the IEEE*, Vol. 78, no. 4, July 1990

Sklar, B. (2001). *Digital Communications,* Prentice-Hall, 2nd Ed, 2001

Turner, L. (May 1991). The Evolution of Featureless Waveforms for LPI Communications, *National Aerospace and Electronic Conference, NAECON* 1991

Glenn, A. B. (1983). Low Probability of Intercept, *IEEE Communications Magazine*, Vol. 21, pp. 26-33, 1983

Gutman, L. L. & Prescott, G. E. (December 1989). System Quality Factors for LPI Communications, *IEEE Aerospace and Electronic Systems Magazine*, Vol. 4, pp. 25-28, 1989

Dillard, G. M. & Dillard, R. A. (November 2001). A Metric for Defining Low Probability of Detection Based on Gain Differences, *IEEE Thirty-Fifth Asilomar Conference on Signals, Systems and Computers*, Vol. 2, pp. 1098-1102, November, 2001

Weeks, G. D.; Townsend, J. K. & Freebersyser, J. A. (1998). A Method and Metric for Quantitative defining Low Probability of Detection, *IEEE Military Communications Conference, MILCOM'98*, 1998

Mills, R. F. & Prescott, G. E. (1995). Waveform Design and Analysis of Frequency Hopping LPI Networks, *IEEE Military Communications Conference, MILCOM'95*, 1995

Mills, R. F. & Prescott, G. E. (July 2000). Detectability Models for Multiple Access Low Probability of Intercept Networks, *IEEE Transactions on Aerospace and Electronic Systems*, Vol. 36, (July 2000), pp. 848-858

Binia, J. (2004). LPI Communication in Channels with Absorption Loss, *IEEE Military Communications Conference, MILCOM'04*, 2004

Wu, P. H. (2005). On Sensitivity Analysis of Low Probability of Intercept (LPI) Capability, *IEEE Military Communications Conference, MILCOM'05*, 2005

Wu, P. H. (2006). Optimal Interceptor for Frequency-Hopped DPSK Waveform, *IEEE the Military Communications Conference, MILCOM'06*, 2006

Burda, K. (2004). The Performance of the Follower Jammer with a Wideband Scanning Receiver, *Journal of Electrical Engineering*, Vol. 55, (2004), pp. 36-38

Gross, F. B. & Chen, K. (April 2005). Comparison of Detectability of Traditional Pulsed and Spread Spectrum Radar Waveforms in Classic Passive Receivers, *IEEE Transactions on Aerospace and Electronic Systems*, Vol. 41, (2005), pp. 746-751

Haykin, S. (February 2005). Cognitive Radio: Brain-Empowered Wireless Communications, *IEEE Journal on selected Areas in Communication*, Vol. 23, (2005), pp. 201-220

NTIA, U.S. frequency allocations. Online available from http://www.ntia.doc.gov/osmhome/allochrt.pdf

Spectrum policy task force report. (2002). *Federal Communications Commission, Tech. Rep. 02-155*, November, 2002

Mitola III, J. & Maguire Jr., G. Q. (1999). Cognitive radio: Making software radios more personal, *IEEE Personal Communications*, Vol. 6, (1999), pp. 13-18

Mitola III, J. (May 2000). Cognitive Radio: An Integrated Agent Architecture for Software Defined Radio, *Ph. D. dissertation, Royal Institute of Technology, Sweden*, May 8, 2000

Jondral, F. K. & Karlsruhe, U. (August 2007). Cognitive Radio: A Communications Engineering View, *IEEE Wireless Communication*, (August 2007), pp. 28-33

Mody, A. N.; Blatt, S. R.; Mills,D. G. & et al. (October 2007). Recent Advances in Cognitive Communications", *IEEE Communication Magazine*, (October 2007)

Cordeiro, C.; Challapali, K.; Birru, D. & et al. (November 2005). IEEE 802.22: the First Worldwide Wireless Standard Based on Cognitive Radios, *Proceeding of 2005 First IEEE International Symposium on New Frontiers in Dynamic Spectrum Access Networks*, pp. 328-337, November 8-11, 2005

Ning, H; Hwan, S. S.; Hak, C. J. & et al. (February 2006). Spectral Correlation Based Signal Detection Method for Spectrum Sensing in IEEE 802.22 WRAN Systems, *Proceeding of 8th International Conference on Advanced Communication Technology*, Vol. 3, pp. 1765-1770, February 20-22, 2006

Cordeiro, C.; Challapali, K. & Birru, D. (April 2006). IEEE 802.22: An Introduction to the First Wireless Standard Based on Cognitive Radios, *Journal of Communicaton*, Vol. 1, No. 1, (April 2006)

Torrieri, D. J. (1986). Fundamental Limitations on Repeater Jamming of Frequency-Hopping Communications, *IEEE Journal on Selected Areas in Communication*, Vol. 7, (1986), pp. 569-575

Felstead, E. B. (October 1998). Follower Jammer Considerations for Frequency Hopped Spread Spectrum, *Proceeding of MILCOM'98*, Vol. 2, pp. 474-478, October 18-21, 1998.

Liao, C. H.; Lee, Z. S.; Tsay, M. K. & Lin, G. J. (2007). Anti-Jamming and LPD/I Performance Trade-off Analysis for Secure Communications, *International Journal of Electrical Engineering*, Vol. 14, No. 6, (2007), pp. 441-449

Liao, C. H.; Tsay, M. K. & Lee, Z. S. (February 2009). Secure Communication System through Concurrent AJ and LPD Evaluation, *Wireless Personal Communications*, Vol. 49, Issue 1, (February 2009), pp. 35-54

Zhao, Y.; Mao, S.; Neel, J.O. & et al. (April 2009). Performance Evaluation of Cognitive Radios: Metrics, Utility Functions, and Methodology, *Proceedings of the IEEE*, Vol. 97 , Issue 1, (April 2009), pp. 642-659

Jayasinghe, L. K. S.; Rajatheva, N. & Latva-aho, M. (2011), Optimal Power Allocation for PNC Relay Based Communications in Cognitive Radio, *IEEE International Conference on Communications (ICC)*, pp. 1-5, 2011

Liu, Y.; Zhao, Z. & Tang, H. (2010). Radio Resource Management between Two User Classes in Cognitive Radio Communication, *Second International Conference on Networks Security Wireless Communications and Trusted Computing (NSWCTC)*, pp. 215-218, 2010

Liang, Y. C.; Chen, K. C.; Li, G. Y. & et al. (September 2011), Cognitive Radio Networking and Communications: An Overview, *IEEE Transactions on Vehicular Technology*, Vol. 60, No. 7, (September 2011), pp. 3386-3407

Advances in Cognitive Radio Systems

Edited by Dr. Cheng-Xiang Wang

ISBN 978-953-51-0666-1
Hard cover, 150 pages
Publisher InTech
Published online 05, July, 2012
Published in print edition July, 2012

How to reference

In order to correctly reference this scholarly work, feel free to copy and paste the following:

Chien-Hsing Liao and Tai-Kuo Woo (2012). Adaptation from Transmission Security (TRANSEC) to Cognitive Radio Communication, Advances in Cognitive Radio Systems, Dr. Cheng-Xiang Wang (Ed.), ISBN: 978-953-51-0666-1, InTech, Available from: http://www.intechopen.com/books/advances-in-cognitive-radio-systems/adaptation-from-transmission-security-transec-to-cognitive-radio-communication

INTECH
open science | open minds

InTech Europe
University Campus STeP Ri
Slavka Krautzeka 83/A
51000 Rijeka, Croatia
Phone: +385 (51) 770 447
Fax: +385 (51) 686 166
www.intechopen.com

InTech China
Unit 405, Office Block, Hotel Equatorial Shanghai
No.65, Yan An Road (West), Shanghai, 200040, China
中国上海市延安西路65号上海国际贵都大饭店办公楼405单元
Phone: +86-21-62489820
Fax: +86-21-62489821

IntechOpen